# Application of NDT method for the concrete girder damaged by chloride

Masahiro Ishida[1], Osamu Usami[2], Akiko Hiroe[3]


## Abstract

Recently corrosion and rupture of the prestressing tendons occur in Japan while the aging of the road bridges progresses because most of them were constructed in Japan's rapid economic growth period. These deteriorations of main parts of bridges has possibility to have a serious influence on the bridges themselves. The technology to investigate and diagnose the condition of constructions adequately is required. In this paper, the current conditions of following things are reported. (1)non-destructive testing (NDT) method, such as X-ray, which is effective to investigation and diagnosis of constructions, (2)the applicability of different fields' NDT technology for bridge inspection.


## Introduction

Many cases of bridges' damage with various deterioration factors are reported while the aging of the road bridges advances because most of them were constructed in Japan's rapid economic growth period. To maintain those bridges reasonably and adequately, the testing technology and evaluation method are required. However, factors of bridges' damage and deformation are diverse. Moreover, load bearing capacity and durability performance are influenced by structural characteristics of bridges, environment, traffic, and so on. It is necessary to stock data of damage to establish the evaluation method of deterioration. PWRI address the research for establishment of the testing technology and evaluation method with NDTs, loading tests and anatomical studies using decommissioned bridges in order to grasp the condition of damaged bridges and load bearing capacity of them. In this paper, NDT to comprehend the condition of the concrete girder which was deteriorated by chloride and developing NDT technology for bridge inspection in different fields are reported.

## Applicability of NDT on decommissioned PC girder

### 1. Research object

This is a pedestrian bridge in Ishikawa, Japan (Photo 1). It was a 2-spaned simple post-tensioned PC T -girder bridge placed 90m from sea. The details of this bridge and standard section were shown on Table 1 and Figure 1. In past 2 times detailed inspection, flaking of concrete was found on girders and it was revealed in chipping inspection that two of the eight prestressing tendons were broken. Therefore, this bridge was judged that

---

[1] Chief researcher, Center for Advanced Engineering Structural Assessment and Research (CAESAR), Public Works Research Institute (PWRI),
[2]Senior researcher, ditto, [3]Researcher, ditto

the replacement was superior than repair from the view point of Life cycle cost. It was replaced after 38 years use.


Photo 1 before replacement

Table 1 details

| | |
|---|---|
| Name | Aimigawa Kaihinkyou Bridge<br>（Pedestrian Bridge） |
| Road | Regional Road<br>Kanazawa-Tazuruhama Line<br>（Ishikawa prefecture） |
| length・span | 44.0m（Span 19.2m＋23.24m） |
| Bridge Type | simple post-tensioned PC T -girder bridge |
| Specifications | Specifications for highway bridges 1968<br>（estimation from completion year） |
| completion year | 1972年 |
| Inspection history | 2007 inspection<br>2009 detailed inspection |

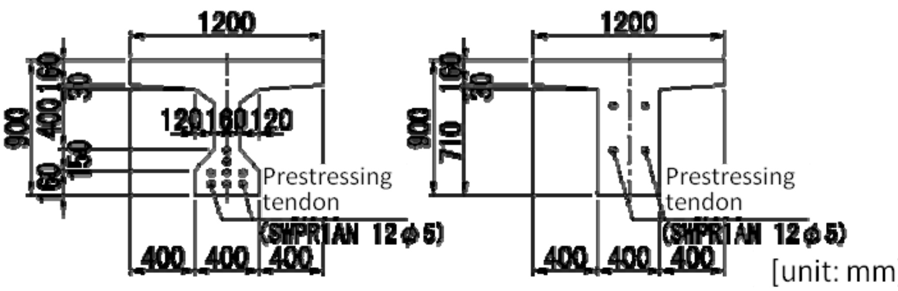


Figure 1 standard section

## 2. Investigation contents

(1) Crack and flaking

Figure 2 indicates the damage condition of the girder before the loading test. The break of prestressing tendons are found on the south side (the right side of the Figure 2 ) of the girder. More cracks and flaking can be found on the south side than the center, and especially on the mountain side and the underside of the girder.

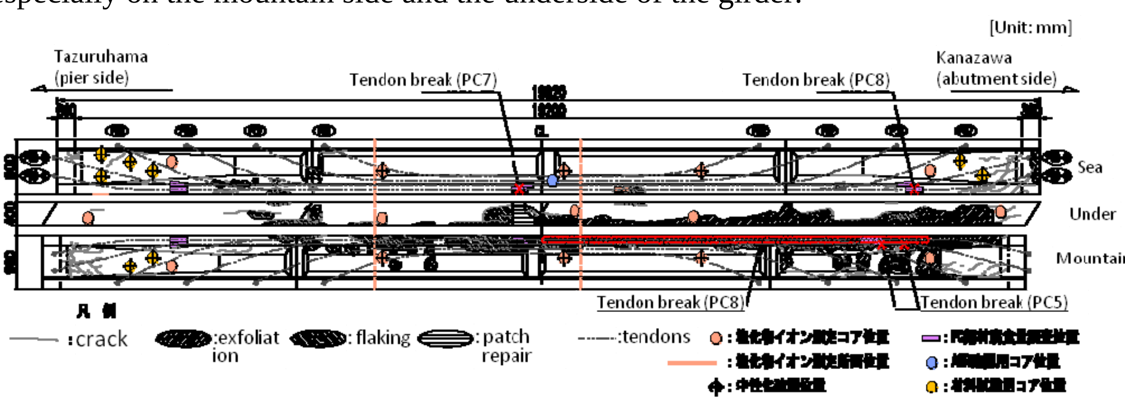


Figure 2 damage condition before loading test

(2) Corrosion of prestressing tendons

Figure 3 represents the decreasing rate of prestressing tendons section at girder ends and center of a span. The rate in the figure shows the average of the cross section of 12 tendons in each sheathes. The significant corrosion was found on the girder end near the abutment, and PC8, lowest sheath on the mountain side, lost itself.

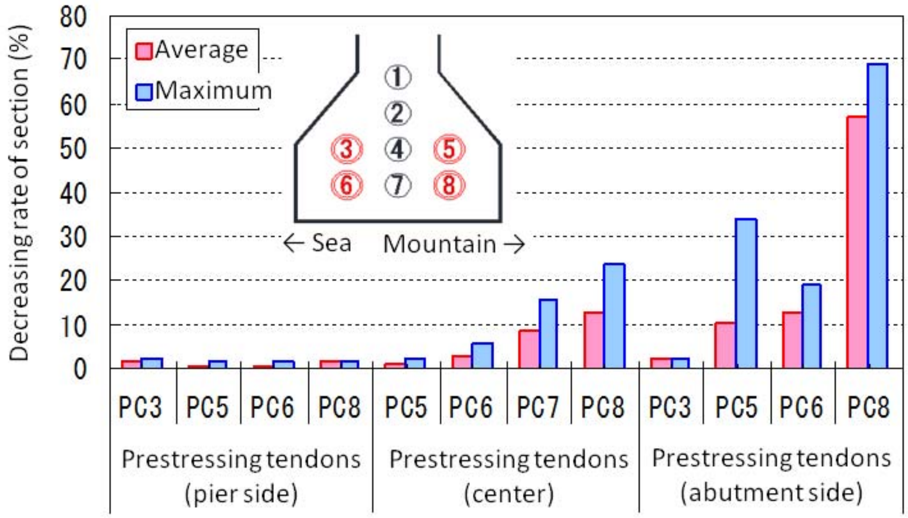


Figure 3 decreasing rate of prestressing tendons section

(3) Corrosion of rebar

Investigation of the corrosion was done in the severe corroded area, south and center parts of the girder. There are flaking of the cover concrete and corrosion of rebars on the south part, the most corroded one. The decreasing rate of section of the lowest rebars, the second lowest rebars and stirrups were measured and it was found that the decreasing rate is 0~60% at the lowest rebars and 0~30% at the second lowest rebars. Stirrups lost their cross section 0~30% at the severely corroded mountain side and 0~10% at the sea side. The decreasing rate of the cross section of Rebars and stirrups were 0~30% in the center part.

(4) Grout sufficiency in sheathes

Insufficiency of grout was found in some sheathes but the condition of grout is good in almost sheathes. The detail is represented in 3.2.

(5) Material strength test

Material strength such as compressive strength, splitting tensile strength and modulus of static elasticity was tested with cores taken from the girder. The results of the average of concrete and steel’s material testing were shown in Table 2.

Table 2 the results of material strength test

(a)Concrete

| | Test value | Standard value (from Specifications for highway bridges) | |
|---|---|---|---|
| compressive strength (N/mm²) | 58.9 | 40 | 60 |
| tensile strength (N/mm²) | 3.16 | 2.69 | 3.53 |
| modulus of static elasticity(kN/mm²) | 21.6 | 31.0 | 35.0 |

(b)Prestressing tendons

| | Rebar(SD295) | | Tendon (SWPR1 AN 12ϕ5) | |
|---|---|---|---|---|
| | test | Standard | test | standard |
| yield strength (N/mm²) | 373 | 295 | 1675 | 1400 |
| tensile strength (N/mm²) | 553 | 440 | 1806 | 1600 |
| modulus of static elasticity(kN/mm²) | 213 | 200 | 203 | 200 |

From the results, the compressive strength and tensile strength recorded greater than the standard value but the modulus of static elasticity was less than standard value. This indicates the influence of the alkali silica reaction (ASR). The tensile strength test was done with the prestressing tendons taken from cut girder end after the loading test. Strain was measured by single direction strain gauges stuck along the tensile axis of the specimens. Stress-Strain curve, yield point, tensile strength and elastic modulus was recorded and all of them were above the specification value.

(6) Neutralization depth

The results of measurement of neutralization depth are shown in Table 3. The neutralization advanced on the mountain side than the sea side relatively. The deepest value among the tested points was about 26 mm at the girder end near the abutment on the mountain side.

Table 3 the results of neutralization depth measurement

| | Compression1 (Sea) | Compression2 (Mt.) | Compression3 (Sea) | Splitting 1 (Sea) | Splitting 2 (Mt.) | Splitting 3 (Sea) |
|---|---|---|---|---|---|---|
| Maximum | 0 | 26 | 0 | 0 | 13 | 0 |
| Minimum | 0 | 6 | 0 | 0 | 4 | 0 |
| Average | 0 | 11 | 0 | 0 | 8 | 0 |

(7) Chlorine content

Chlorine content was tested by the core taken from the girder. The chlorine content distribution was drawn in Figure 4. Chlorine content was low on the mountain and the sea side in the pier side which was less damaged. On the other hands, on the mountain side in the center part, the mountain side and the underside in the abutment side, which were significantly damaged, contained a lot of chloride ions. The chlorine content was more than 1.2 kg/m3 at the prestressing tendons in those portions. The chlorine content near surface is low in the same portion. The neutralization depth on each mountain side, the maximum value of point equally dividing the circumference of each core into 8 parts, was shown in Figure 4 and it could be found the relation between the neutralization depth and the chlorine content near surface. It is considered that this phenomenon occurred because of the concentration of chloride ions by neutralization.

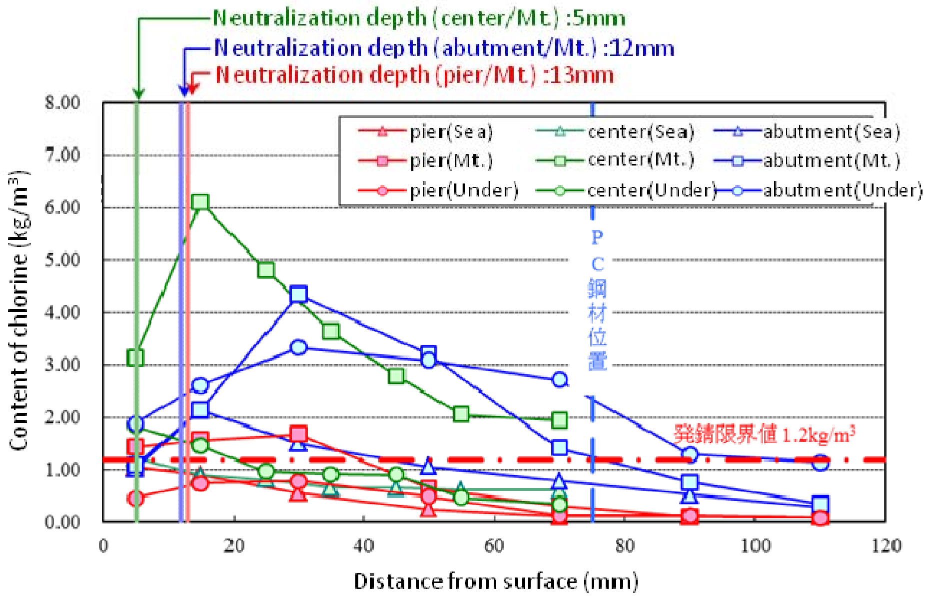


Figure 4 distribution of chlorine content by potentiometric titration

(8) Loading test

Loading tests were done 3 times, the bending test at the center of the girder and the shearing test at both girder end, as shown in Figure 5. Hereafter, the shearing test at the origin side is represented as "Shearing test 1" , the shearing test at the terminus side is represented as "Shearing test 2" and the bending test is described as "Bending test". The results of the loading tests are shown in Figure 6. In Shearing test 1, the indication of yield of prestressing tendons appeared in the load-displacement curve after shear cracking. The maximum load in Shearing test 1 is 500 kN. Load was removed in order not to influence to Shearing test 2 after 500kN was recorded. Shearing test 2 showed similar behavior to Shearing test 1 before flexural cracking occurred. After that, the displacement became greater than Shearing test 1 and Maximum load 575 kN was recorded.

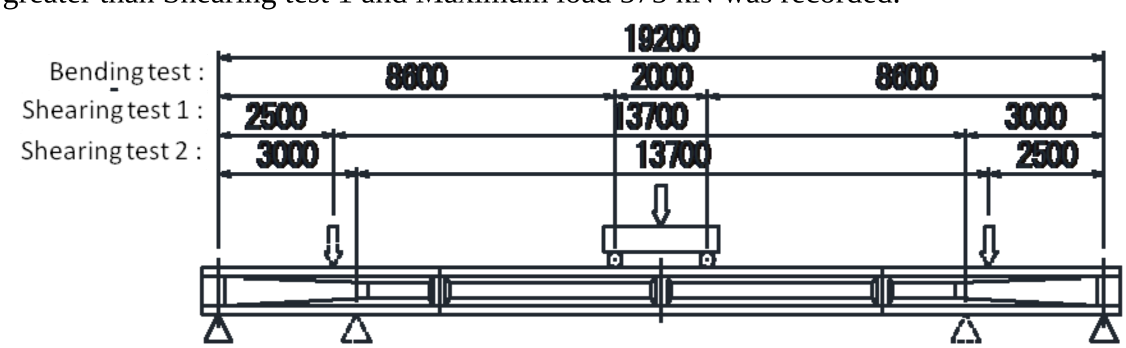


Figure 5 the way of loading test

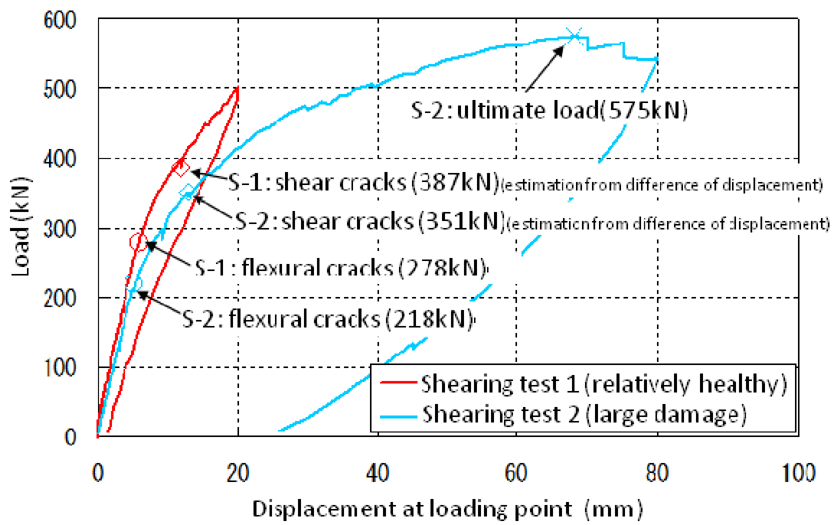


Figure 6 load-displacement curve (shearing test)

## 3. Application of NDT

### 3.1 The outline of NDT

The applicability of following NDT method was examined.

(1) X-ray transmission method (Photo 2)

The grout sufficiency was investigated by X-ray. X-ray radiography was also applied the place where the breaks of prestressing tendons were found by a check in service and the corrosion of rebar was shown in visual survey. The applicability of X-ray transmission method was confirmed.

(2) Vibration measurement (Photo 3)

Before and after Shearing test 1, the vibration characteristics were investigated by the measurement of micro-tremor and vibration by impulse excitation. The impulse excitation was occurred by 10 kg sand bag and 8 servo-type accelerometers measured from primary to third mode of natural frequency. The change of natural frequency by damage condition of specimen by loading test was confirmed.

(3) Full-field optical measurement (Photo 4)

Displacement and strain of concrete were measured at the lower flange side and the web near the loading point during loading test by utilizing full-field optical measurement equipment developed by Nagasaki University and Saga University. The measurement was done by a camera and a scanner. In this paper, the results of the measurement of the digital image correlation method (DICM) using a camera during Shearing test 2 was reported.

(4) Measurement using a laser (Photo 5)

The comparison between a contact-type displacement gauge and the noncontact method, which is the displacement measuring method using a laser irradiated to the target on the test body. While this comparison investigation, the vibration measurement was also done. From those 2 investigations, the applicability was examined.

(5) Chloride ion measurement by X-ray fluorescence (Photo 6)

The distribution of chloride ion on the section and the side was measured utilizing X-ray fluorescence device.

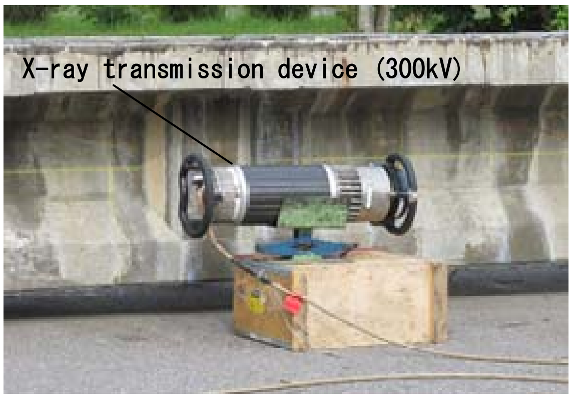


Photo 2  X-ray transmission method


Photo 3 Vibration measurement

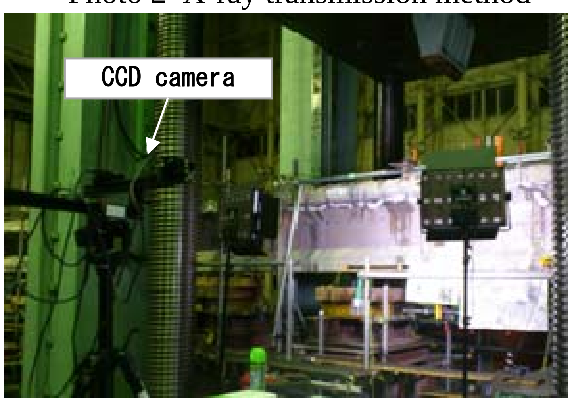


Photo 4 Full-field optical measurement

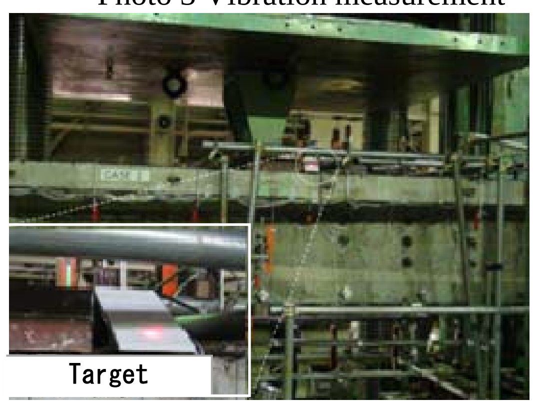


Photo 5 Measurement using a laser

Photo 6 X-ray fluorescence device

3.2 The results of applicability examination

(1) X-ray transmission method

The results of the grout sufficiency check are shown in Figure 7.

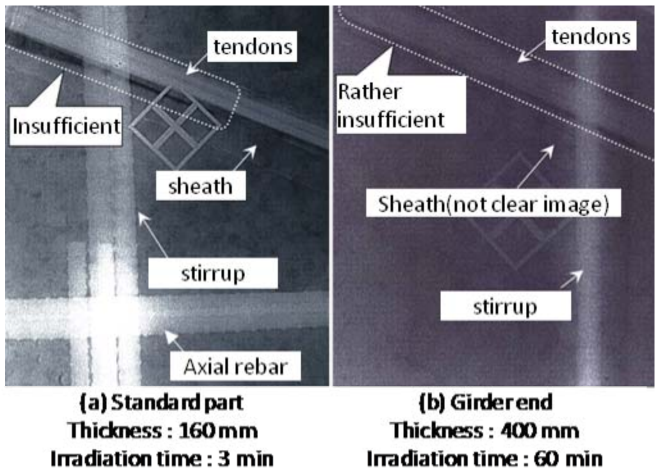


Figure 7 the condition of grout filmed using X-ray

Insufficiency of grout because of a flow a head phenomenon or bleeding was found in some place but the condition of grout was relatively good. The required time to get a clear image is approximately 3 minutes when the thickness of the specimen is around 160mm. But when the thickness is 400mm at the girder end, a clear image could not be taken by even 1 hour irradiation. The trial of X-ray transmission method was done at the point where the breaks or corrosion of steel was found but a significant results were not obtained. In the anatomical study, the sufficiency of grout was investigated from the sheathes, taken out from the girder and cut into round slices (Figure 8). The results were same as NDT.

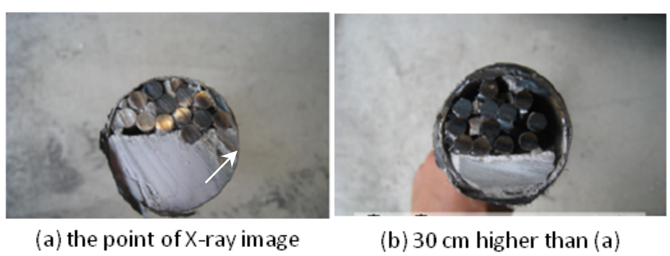


Figure 8 the condition of grout (cut sheath)

(2) Vibration measurement

The results of the natural frequency measurement done before and after Shearing test 1 are shown in Table 4. The micro-tremor was also measured but the high-order mode was not found. The primary and secondary mode did not change in the frequency by impulse excitation but 8% decrease was identified in the third mode. This is because of the stiffness reduction by cracking.

Table 4 The results of the natural frequency

| Mode order | Loading test | Natural frequency (Hz) | |
|---|---|---|---|
| | | micro-tremor | impulse excitation |
| 1 | Before | 6.694 | 6.378 |
| | After | 6.458 | 6.353 |
| | Rate | 0.95 | 1.00 |
| 2 | Before | 21.301 | 21.276 |
| | After | 21.130 | 21.047 |
| | Rate | 0.99 | 0.99 |
| 3 | Before | Undeterminable | 57.363 |
| | After | Undeterminable | 52.953 |
| | Rate | — | 0.92 |

(3) Full-field optical measurement (Photo 4)

The results of the comparison among DICM, contact-type displacement gauge and strain gauge is shown in Figure 9. In Figure 10, the distribution of strain from the full-field optical measurement is drawn and the crack found by visible check is also in the figure with a black line. The full-field optical measurement captured displacement and strain generally. Strain gauge is only able to measure a point but the full-field optical measurement is able to capture strain planarly. Development of this method is expected.

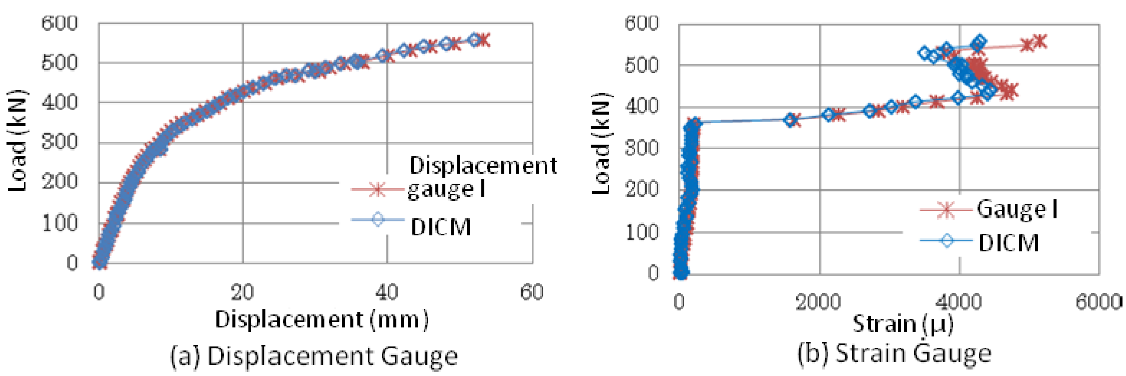


Figure 9 comparison of measurement

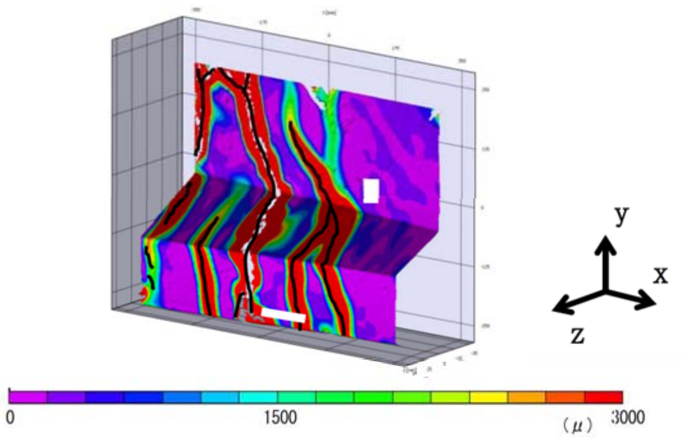


Figure 10 distribution of strain (load: 520kN)

(4) Measurement using a laser

The comparison of the displacement measurement by laser and contact-type gauge is represented in Figure 11.

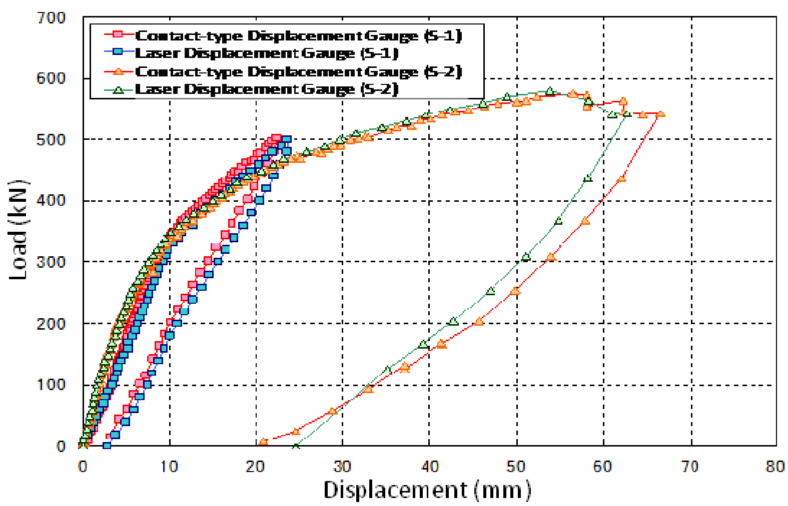


Figure 11 the results of comparison

In Shearing test 1, the result of laser generally coincides with that of contact-type displacement gauge and displacement motion was captured relatively accurately. In Shearing test 2, the results generally coincides up to the maximum load but 3~4mm difference appeared during the load removing. The cause of this difference is considered that a gap occurred on either gauge because of damage by loading.

(5) Chloride ion measurement by X-ray fluorescence

The calibration curve which is used to quantify from X-ray intensity to chlorine content was compensated for this investigation. The results of measurement by X-ray fluorescence using the compensated calibration curve is shown in Figure 12.

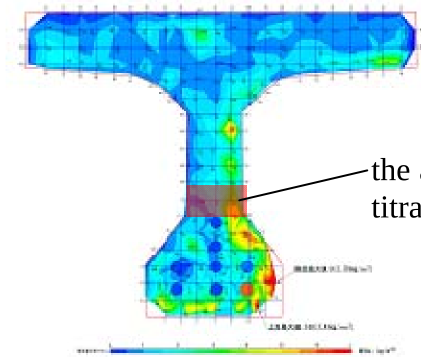


Figure 12 The results of measurement by X-ray fluorescence

Figure 13 represents the comparison between measurement by X-ray fluorescence and potentiometric titration of the core taken from near the place of X-ray fluorescence measurement. Interrelation can be found generally but the result of X-ray fluorescence records higher value than that of potentiometric titration when the chlorine content is low. This reason is conceivable that the X-ray fluorescence measurement was done on the mortar with avoiding aggregate, or the calibration curve was compensated with powder sample including coarse aggregate. The side of the specimen was also measured and the side contain lower chloride ion than the section at no flaking area. X-ray fluorescence measures very thin area, tens of $\mu$m from the surface. If the neutralization occurs in the investigation area, the measured value become low because of concentration of chloride ion. It need to notice when X-ray fluorescence device is used in a field.

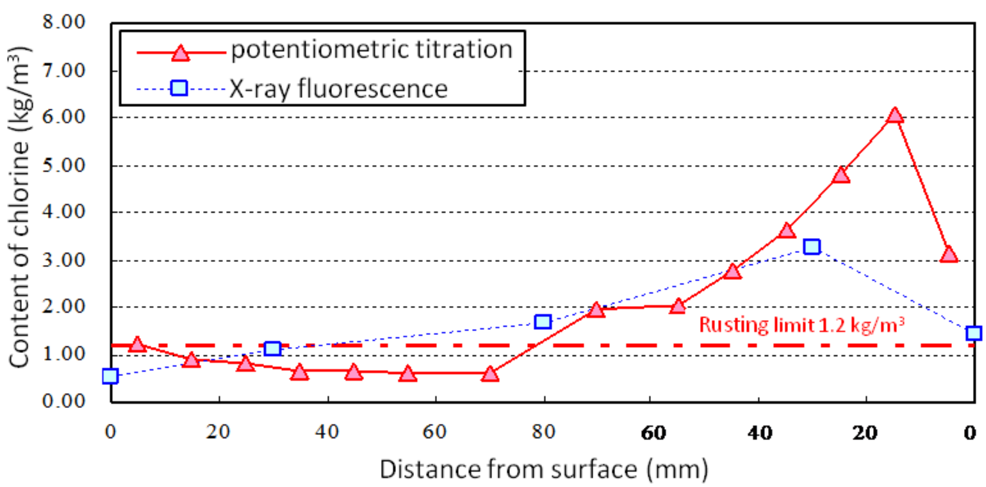


Figure 13 the result of measurement by X-ray fluorescence

### 3.3 Summary

The summary of applicability examination of NDT is followings.

(1) X-ray transmission method has a limit of measurable thickness of parts and significant results of application to breaks and corrosion of tendons could not be obtained from this investigation.

(2) The vibration measurement by impulse excitation using servo-type accelerometers revealed that high-order mode has a possibility to detect damage.
(3) The full-field optical measurement is able to capture strain planarly while strain gauge is only able to measure a point.
(4) The laser could capture displacement motion relatively accurately up to the maximum load. But in vibration measurement, there is a limit of its resolution for now and the measuring error occurred.
(5) The measurement of chloride ion by X-ray fluorescence is partly available but the measured value is low on the neutralized concrete surface. It need to notice when X-ray fluorescence device is used in a field.

**The applicability of NDT technology for bridge inspection in different fields**

1. Development of technology for concrete bridge inspection by high-power X-ray source

To evaluation of load bearing capacity of existing concrete bridges, it is necessary to grasp the condition of cracks in concrete, the position of rebar and prestressing tendons, their diameter, and their condition of corrosion. X-ray transmission method, one of the NDT method, is able to get these information. Furthermore, by using computer tomography (CT) technology, it has a possibility to visualize complicated internal structure of bridges. However, the problems of X-ray source which is used in bridge inspection now are that it is restricted its power to 300 keV, limit of application is 30~40 cm thick, it takes time to film when the parts are thick. Because of those problems, current NDT technology has its limit. Concrete bridge inspection technology by high-power X-ray source is now being developed in cooperation with Tokyo University. In Japanese law which limits the use of X-ray, it is approved to use X-ray source to 4 MeV only in bridge inspection. Therefore, the portable 3.95 MeV X-band linac X-ray sources developed by Uesaka et.al is focused. Photo 7 shows the exterior of the portable 3.95 MeV X-band linac X-ray sources and Figure 14 shows the image of the linac.

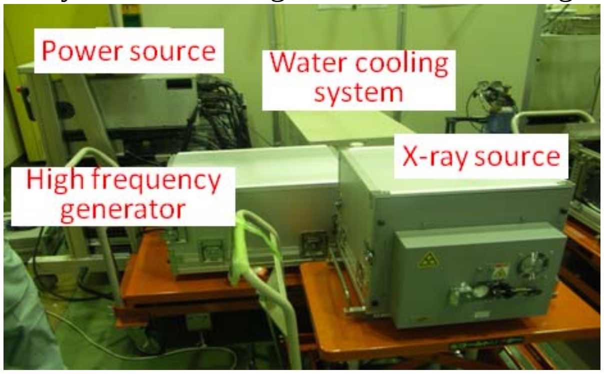

Photo 7 the portable 3.95 MeV X-band linac X-ray sources

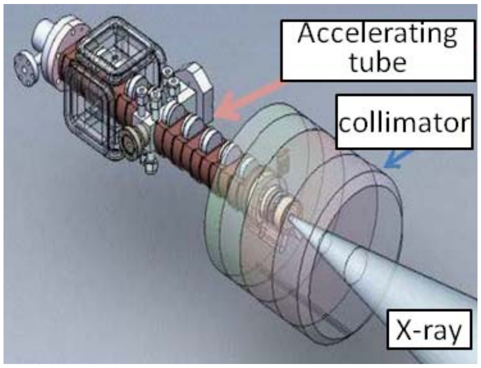

Figure 14 the image of the linac

The portable 3.95 MeV X-band linac X-ray sources consists of X-ray source, radio frequency source, electric power source and water-cooled device. Its weight is less than 200kg in order to be able to mount on the bridge inspection vehicle, and it is lighter than other high-power devices. To confirm the basic performance of the device, The part of the lower flange of the decommissioned PC girder (Photo 8) was x-rayed.

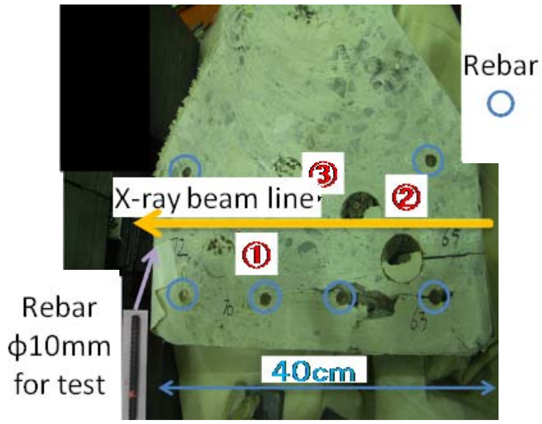


Photo8 the part of PC girder

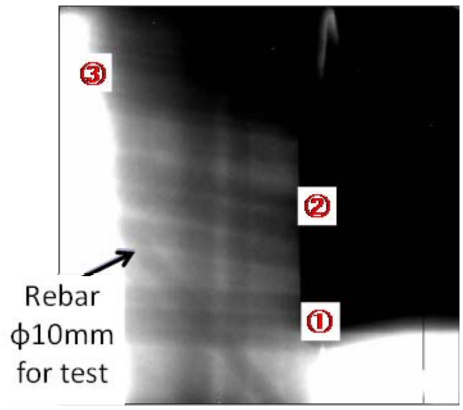


Photo9 X－ray image (expose time: 1 sec)

This part is 40 cm thick. It takes approximately 1 hour to x-ray by former X-ray devices but Photo 9 could get an image with only several seconds. This girder adopted a post-tension system and 12 prestressing tendons which are 7mm in diameter are settled in each sheath. In each sheath, only 3 prestressing tendons is able to recognize from Photo 9 because this image is taken from one direction. However this X-ray device can take plural images with different angles in short time. Therefore, CT technology is developed in parallel with the development of device itself for improvement of accuracy.

## 2. Development of technology for concrete bridge inspection by neutron beam

Technology for permeation observation by neutron beam is being developed in cooperation with RIKEN, Institute of Physical and Chemical Research, in Japan. X-ray interacts with electrons in atoms, which cause the resistance of X-ray permeation when the atomic number gets larger. But neutron beam has no electrical charges and interacts with atomic nucleus, so that the permeation is different by atomic nucleus. For example, neutron beam can permeate steel which X-ray is hard to, while neutron is hard to permeate hydrogen atom. Using this characteristics, neutron beam have been utilizes in the moisture metering of ready-mixed concrete force-feeding pipe. The example of neutron radiography is shown in Figure 15.

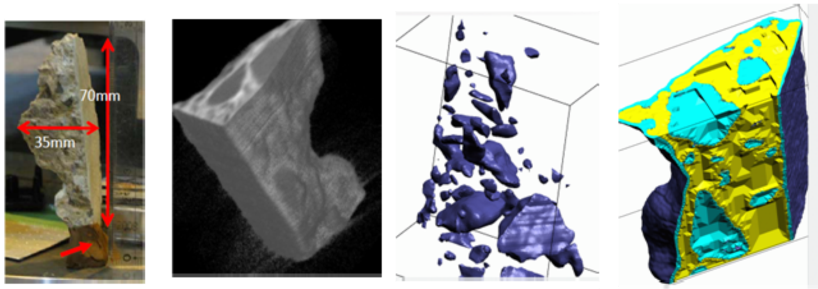


A) Concrete specimen B) Surface image C) Aggregate D) Cement &aggregate

Figure 15 example of neutron radiography

Figure 15 expresses the 3D image of concrete test piece, which is 70mm long and 35mm in maximum thickness, analyzed with 300 images filmed per 0.6 degrees while turning 180 degrees using CT technology. These represent the internal structure of the concrete by separating aggregate and cements. Using characteristics that neutron beam is attenuated by water, there is an example that moisture transport in cracks of concrete was visualized. The image of permeation observation device using neutron beam for bridge inspection is shown in Figure 16. Currently, the portable neutron source system is prepared in RIKEN and it is possible to take an image of small-scale bridge parts.

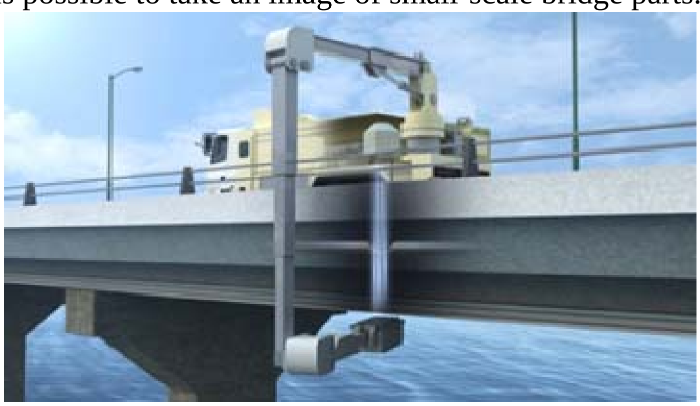

Figure 16 image of portable neutron imaging device (source: RIKEN)

3. Summary

The applicability of high-power X-ray and neutron beam was considered from the perspective of detection of cracks in concrete and corrosion of rebars or prestressing tendons using decommissioned bridge parts. As a result, it was revealed that they have a possibility to apply to onsite NDT. The development for practical use of these technology are expected.

## **Conclusion**

Application of NDT is expected in order to diagnose the aging infrastructure, but there are still many problem to solve. Henceforth, using technology of not only civil engineering but also other fields, development of NDT will be advanced.